


## Article

# Genome-Wide Identification of CBL Gene Family and RNA-Seq Analysis Under Alkaline Stress in Poplar

Hanzeng Wang <sup>1,†</sup> , Juan Wu <sup>1,†</sup>, Zhixin Ju <sup>1</sup>, Jingli Yang <sup>2,\*</sup> and Xue Leng <sup>1,\*</sup>

<sup>1</sup> College of Agriculture, Jilin Agricultural Science and Technology University, Jilin 132101, China; hzwang0@163.com (H.W.); einewwj1001@163.com (J.W.); juzhixin@jlnku.edu.cn (Z.J.)

<sup>2</sup> State Key Laboratory of Tree Genetics and Breeding, Northeast Forestry University, Harbin 150040, China

\* Correspondence: yifan85831647@nefu.edu.cn (J.Y.); lengxue19910514@163.com (X.L.)

† These authors contributed equally to this work.

**Abstract:** Calcium ions (Ca<sup>2+</sup>) play a crucial role as a key messenger in various adaptive and developmental processes. In plants, the calcineurin B-like protein (CBL) family is a unique calcium sensor, which plays a key role in regulating plant growth and development as well as responding to external environmental stimuli throughout the Ca<sup>2+</sup> signaling pathway. However, the CBL gene family in poplar has not been systematically described. In this study, thirteen CBL genes were identified from the *Populus trichocarpa* genome using bioinformatics methods. Multiple sequence alignment showed that all PtrCBLs contained four conserved EF-hand domains. Promoter *cis*-acting elements revealed that PtrCBL promoters contained at least one abiotic-related or hormone response element. A protein–protein interaction network revealed that PtrCBLs interacted with various CIPK proteins to participate in growth and development or respond to environmental stimuli in poplar. Transcriptome data demonstrated that numerous *PsnCBLs* were involved in the response to alkaline stress in *Populus simonii* × *Populus nigra*. RT-qPCR and RNA-seq analyses implied that *PsnCBLs* exhibited complex expression patterns in poplar under alkaline stress at different time points. These results provide comprehensive information for future research on the CBL gene function and lay a research foundation for studying alkaline stress in poplar.

**Keywords:** calcineurin B-like; bioinformatics; RNA-seq; alkaline stress; poplar



Academic Editor: Om P. Rajora

Received: 19 December 2024

Revised: 9 January 2025

Accepted: 21 January 2025

Published: 22 January 2025

**Citation:** Wang, H.; Wu, J.; Ju, Z.; Yang, J.; Leng, X. Genome-Wide Identification of CBL Gene Family and RNA-Seq Analysis Under Alkaline Stress in Poplar. *Forests* **2025**, *16*, 200. <https://doi.org/10.3390/f16020200>

**Copyright:** © 2025 by the authors. Licensee MDPI, Basel, Switzerland. This article is an open access article distributed under the terms and conditions of the Creative Commons Attribution (CC BY) license (<https://creativecommons.org/licenses/by/4.0/>).

## 1. Introduction

Plants consistently encounter diverse adverse ecological stress factors, including extreme temperatures, drought, and saline-alkali stress during growth and development [1]. Calcium ion (Ca<sup>2+</sup>), functioning as second messengers, can detect and transmit external stress signals within plants, as well as participate in various signal transduction processes [2]. When plants perceive external stimuli, the Ca<sup>2+</sup> concentration in the cytoplasm rapidly increases. The free Ca<sup>2+</sup> binds to calcineurin B-like protein (CBL), a Ca<sup>2+</sup> sensor, to regulate downstream target proteins, triggering physiological changes in plants and contributing to the response to external environmental stimuli [3]. To date, four types of Ca<sup>2+</sup> receptors have been identified, including calmodulin protein (CaM), calmodulin-like proteins (CML), calcium-dependent protein kinase (CDPK), and CBL [4]. Previous research has demonstrated that CBL members possess a distinct ability to bind Ca<sup>2+</sup>, which can bind to the serine/threonine of CIPK and activate target proteins. This activation, in turn, catalyzes the phosphorylation of various target proteins to generate feedback in response

to stress [5]. This pathway regulates multiple processes, including defense responses, ion homeostasis, and gene expression [6].

Previous studies have established that CBL proteins contain four elongation factor hand (EF-hand) structures, which are conserved domains capable of binding  $\text{Ca}^{2+}$  [6]. Analysis of CBL amino acid sequences in *Arabidopsis thaliana*, revealed variability in the number of typical EF-hand domains. Specifically, AtCBL6, AtCBL7, AtCBL8, and AtCBL10 contain only one typical EF-hand domain, while AtCBL1 and AtCBL9 possess two. Notably, AtCBL2, AtCBL3, AtCBL4, and AtCBL5 lack typical EF-hand domains [2]. The diversity in domains among CBL proteins may result in distinct  $\text{Ca}^{2+}$ -binding capabilities, providing a foundation for CBLs' response to various stimulus signals that affect  $\text{Ca}^{2+}$  concentration [7]. Furthermore, CBL proteins also contain an FPSF motif. The spatial structure of this motif enables specific recognition and binding to the corresponding structural regions on interacting protein kinases [8].

The first CBL gene was identified in *Arabidopsis thaliana* [9]. To date, the CBL gene family has been characterized across diverse species, including *Oryza sativa* [10], *Solanum lycopersicum* [11], *Gossypium hirsutum* Linn [12], *Vitis vinifera* [13], and *Ananas comosus* [14]. CBLs play crucial roles in plant growth and development processes, such as seed germination and pollen tube germination, as well as in response to abiotic stresses, including high salinity, low temperature, and drought [15,16]. The expression patterns of CBL transgenic plants vary under different abiotic stresses, thereby modulating plant stress tolerance [15]. Previous studies have demonstrated that CBL genes enhance stress tolerance in various plants. The roles of CBLs in regulating abiotic stresses, particularly drought and salt stress, have been well-documented. Overexpression of CBL1, CBL9, CIPK1, and CIPK6 has been shown to increase drought tolerance in *Arabidopsis* [17]. Heterologous expression of *Ac-CBL1* (*Ananas comosus* CBL11) and *AcCIPK5* enhances tolerance to salt, osmotic, and cold stresses in transgenic *Arabidopsis* [14,18]. *GmCBL1-OE* lines improve alkaline tolerance in transgenic soybeans by regulating redox reactions [19]. Conversely, *atcbl10* mutation leads to increasing salt sensitivity in *Arabidopsis* [20]. AtCBL2 and AtCBL3 participate in growth, embryo, and seed development, as well as response to high-concentration ion stress in *Arabidopsis* [7]. AtCBL2 responds to high alkaline (high pH value) stress by binding to AtCIPK11 [21]. AtCBL4 promotes the antiporter AtSOS3 to pump excessive  $\text{Na}^+$  out of cells, ensuring intracellular  $\text{Na}^+$  balance by interacting with AtCIPK24 [22].

The distribution area of saline-alkali land in Northeast China is approximately 765  $\text{hm}^2$  [23]. *P. simonii*  $\times$  *P. nigra*, a hybrid poplar characterized by its fast growth and strong adaptability to the external environment, has been widely used for afforestation and commercial forestry in Northeast China. The genome-sequenced tree species provide a research foundation for the functional study of the CBL gene in *P. simonii*  $\times$  *P. nigra*. In this study, *PtrCBLs* were identified and analyzed from *P. trichocarpa* through bioinformatics methods, including analyses of protein structures, evolutionary relationships, chromosome localization, protein interaction networks, and protein phosphorylation site prediction. Transcriptome technology, serving as a powerful bioinformatics tool, plays a crucial role in contemporary biological research. We employed RNA-seq and RT-qPCR techniques to analyze the expression patterns of *PsnCBLs* in *P. simonii*  $\times$  *P. nigra* under different alkaline concentration treatments. Our predictions and experimental results will provide a preliminary basis for further functional research on CBL genes under alkaline stress in *P. simonii*  $\times$  *P. nigra* and other tree species.

## 2. Materials and Methods

### 2.1. Identification of CBL Genes in *P. trichocarpa*

To identify the CBL members in *P. trichocarpa*, we obtained 10 *AtCBL* genes from the Arabidopsis Information Resource (TAIR10) website (<https://www.arabidopsis.org/>, accessed on 19 November 2024). The NCBI-Blast website (<https://blast.ncbi.nlm.nih.gov/Blast.cgi>, accessed on 19 September 2024) and the Phytozome database (<https://phytozome-next.jgi.doe.gov/>, accessed on 19 September 2024) were utilized to perform a blast search against the *P. trichocarpa* genome using the amino acid sequences of 10 *AtCBLs* [24]. The *AtCBL* gene ID, protein sequences, and sequence similarity between *P. trichocarpa* and *Arabidopsis* are listed in Supplementary Table S1. Candidate *PtrCBL* family genes were analyzed to confirm the presence of the conserved PF13499 (EF-hand domain pair) in amino acid sequences using the Pfam database (<http://pfam.xfam.org/>, accessed on 19 September 2024) and the SMART database (<http://smart.embl-heidelberg.de/>, accessed on 19 September 2024) [25]. The physicochemical properties of *PtrCBLs* were calculated using the ExPasy website (<https://web.expasy.org/protparam/>, accessed on 19 September 2024) [26]. The number of *PtrCBL* amino acids was directly obtained from the Phytozome database. The TMHMM-2.0 website (<https://services.healthtech.dtu.dk/services/TMHMM-2.0/>, accessed on 3 January 2025) was employed to predict the transmembrane structural domain. Subcellular localization prediction was conducted using the Cell-PLoc 2.0 website (<http://www.csbio.sjtu.edu.cn/bioinf/plant-multi/>, accessed on 19 September 2024) [27]. The chromosome localization information of *PtrCBLs* was obtained from the Phytozome database through the corresponding gene ID. Visual chromosome localization of *PtrCBLs* was carried out using the MG2C v2.1 online tool ([http://mg2c.iask.in/mg2c\\_v2.1/index.html](http://mg2c.iask.in/mg2c_v2.1/index.html), accessed on 21 September 2024) and Adobe Illustrator v28.6 [28,29].

### 2.2. Phylogenetic Analysis and Multiple Sequence Alignment

We obtained 15 *GmCBL* IDs, as referenced in a previous study, and acquired amino acid sequences from the Phytozome database [19]. The amino acid sequences of 13 *PtrCBLs*, 10 *AtCBLs*, and 15 *GmCBLs* were aligned using ClustalW in MEGA11 (v11.1.10) [30]. The Neighbor-Joining method was employed to construct the phylogenetic tree with 1000 bootstrap replications. We utilized the Gene Structure Display Server website to visualize the distribution of introns and exons using genomic sequences and coding sequences [31]. The Multiple EM for Motif Elicitation (MEME, v5.5.7, <https://meme-suite.org/meme/>, accessed on 25 September 2024) online tool was used to search for conserved motifs [32]. The final visualized results were displayed using Adobe Illustrator v28.6.

### 2.3. Analysis of Promoter *cis*-Acting Elements

The promoter regions of *PtrCBLs* were defined as 2000 bp upstream of the coding sequence, including the 5'UTR. The PlantCARE online tool (<https://bioinformatics.psb.ugent.be/webtools/plantcare/html/>, accessed on 25 September 2024) was employed to analyze promoter *cis*-acting elements [33]. This study primarily focused on identifying promoter *cis*-acting elements associated with hormones (ABA-, MeJA-, GA-, and SA-related) and abiotic stress (low temperature- and drought-related). The IBS software (v1.0.1) was utilized to visualize the localization of the *PtrCBLs* promoter *cis*-acting elements.

### 2.4. Prediction of Phosphorylation Sites

The amino acid sequences of *PtrCBLs* were used as the input for the prediction of phosphorylation sites using the *PtrNetPhos* 3.1 website (<https://services.healthtech.dtu>

[dk/services/NetPhos-3.1/](https://services/NetPhos-3.1/), accessed on 30 September 2024) [34]. In the parameter settings, the analysis focused on identifying serine, threonine, and tyrosine phosphorylation sites. Results with a combined score exceeding 0.5 were deemed reliable. The findings were subsequently visualized using GraphPad Prism 10.

### 2.5. Protein Tertiary Structure and Interaction Network

The protein tertiary structure of the PtrCBLs was analyzed using the SWISS-MODEL online platform (<https://swissmodel.expasy.org/interactive>, accessed on 30 September 2024). The alignment parameters were configured to include 50 models. To predict interacting proteins, the 13 PtrCBL amino acid sequences were input into STRING (version: 12.0). On the input page, “*Populus trichocarpa*” was designated as the species on the input page. The parameter included, “full STRING network”, “Network type”, and “Textmining, Experiments, Databases, Co-expression, Neighborhood, Gene Fusion, Co-occurrence” as the “active interaction sources”. The “minimum required interaction score” was established at 0.40. Cytoscape (version: 3.10.2) was utilized to visualize the protein–protein interaction results.

### 2.6. Plant Materials, Alkaline Stress and RNA-Seq Analysis

The branches of two-year-old *P. simonii* × *P. nigra*, cultivated at Jilin Agricultural Science and Technology University, Jilin, China, were cut into 10 cm cuttings and inserted into flowerpots containing a substrate mixture (humus soil:vermiculite:perlite = 5:3:2) for cultivation in April 2024. The cultivation was conducted at  $24 \pm 2$  °C, with a 16-h light period (5000 Lux) and an 8-h dark period in a greenhouse. Plants were irrigated with Hoagland nutrient solution, applying 250 mL to each flowerpot twice weekly. After 4 weeks of culture, *P. simonii* × *P. nigra* exhibiting consistent growth were selected for alkali stress treatment. The alkali stress solution comprised  $\text{Na}_2\text{CO}_3$  and  $\text{NaHCO}_3$  in a 1:1 ratio. Hoagland nutrient solutions containing three different alkali concentrations, including 0 mmol/L, 50 mmol/L (low concentration), and 200 mmol/L (high concentration), were prepared to irrigate the *P. simonii* × *P. nigra*. The group with 0 mmol/L (Hoagland nutrient solution without  $\text{Na}_2\text{CO}_3$  and  $\text{NaHCO}_3$ ) served as the control. Each flowerpot received 250 mL of solution, with the control group receiving an equal volume of water concurrently. Irrigation occurred twice weekly, with three biological replicates per treatment group. Leaves of *P. simonii* × *P. nigra* were sampled at 7 d and 14 d after each treatment, respectively, rapidly frozen in liquid nitrogen, and stored at  $-80$  °C for subsequent analysis.

RNA sequencing was conducted by BioMarker Technologies Company (Beijing, China). The experimental procedure involved constructing mRNA libraries for each *P. simonii* × *P. nigra* sample under alkaline stress, followed by sequencing using the Illumina Novaseq platform. Upon completion, the raw data underwent quality assessment. This process involved removing reads containing adapter sequences, poly-N fragments, and those of poor quality, ensuring high-quality data for subsequent analyses and guaranteeing accurate and reliable results. HISAT2 software (version 2.2.1) was employed to align the high-quality reads with the *P. trichocarpa* reference genome, ensuring accurate read localization on the genome. The feature Counts software (version 1.5.0) was used to quantify the aligned reads corresponding to each gene, with the FPKM value serving as the standard quantitative unit for gene expression levels. Differentially expressed genes (DEGs) were identified using the DESeq2 analysis tool. The screening criteria for DESeq2, differentially expressed genes (DEGs) were as follows: genes with a false discovery rate (FDR) below 0.01 and an absolute value of  $\log_2$  (fold change) not less than 1.2 [35]. The processed data were visualized as expression heatmaps using GraphPad Prism 10, with expression levels calculated by  $\log_2$  (FPKM).



### 2.7. RNA Extraction and RT-qPCR

Fresh leaves from each treatment were harvested, frozen in liquid nitrogen, and stored at  $-80\text{ }^{\circ}\text{C}$  until RNA isolation. High-quality RNA was extracted from *P. simonii*  $\times$  *P. nigra* using the RNeasy Plant Mini Kit (Qiagen, Dusseldorf, Germany), following the manufacturer's instructions. RNA quality was assessed using 1.2% agarose gel electrophoresis and a nucleic acid concentration analyzer (Nanodrop 2000, Thermo Scientific, Waltham, MA, USA). The results of the RNA quality check are provided in Supplementary Table S2 and Supplementary Figure S1. RNA was reverse transcribed to cDNA using the TransScript<sup>®</sup> One-Step gDNA Removal and cDNA Synthesis SuperMix kit (TransGen, Beijing, China). RT-qPCR was performed using a 10  $\mu\text{L}$  reaction system with AceQ<sup>®</sup> Universal SYBR qPCR Master Mix kit (Vazyme, Nanjing, China). The RT-qPCR conditions were as follows: initial denaturation at  $95\text{ }^{\circ}\text{C}$  for 7 min, followed by 35 cycles of  $95\text{ }^{\circ}\text{C}$  for 15 s,  $60\text{ }^{\circ}\text{C}$  for 20 s, and  $72\text{ }^{\circ}\text{C}$  for 30 s. The qTOWER 3G Cyclor (Analytik Jena, Jena, Germany) was used for the RT-qPCR reaction, and the relative expression patterns of the *PsnCBL* genes were calculated using the  $2^{-\Delta\Delta\text{Ct}}$  method. Nine *PsnCBL* (*PsnCBL2*, 3, 4, 5, 6, 8, 10, 12, and 13) with relatively high FPKM values in the transcriptome were selected for primer design. Primers were designed within the 5'UTR using the NCBI Primer-Blast online tool. The *PsnActin* gene (GenBank ID: XM\_002298946) served as the internal reference gene [36]. All primer information for *PsnCBL* and *PsnActin* is provided in Supplementary Table S3.

### 2.8. Statistical Analysis

A two-tailed Student's *t*-test method in SPSS 22.0 software was used to verify the results of RT-qPCR. An asterisk (\*) represents a significant difference ( $p < 0.05$ ), and double asterisks (\*\*) represent an extremely significant difference ( $p < 0.01$ ). All data were obtained from at least three biological replicates. Subsequently, the data are presented in the form of means  $\pm$  standard deviation (SD).

## 3. Results

### 3.1. Identification of the CBL Genes in *Populus trichocarpa*

In this study, 13 *PtrCBL* family genes in *P. trichocarpa* were identified and named *PtrCBL1-PtrCBL13*. Physicochemical property analysis of the *PtrCBLs* revealed amino acid sequences ranging from 213 aa to 254 aa. *PtrCBL8* exhibited the largest molecular weight at 29.24 kDa, followed by *PtrCBL4* at 27.83 kDa, while the remaining 11 *PtrCBL* genes ranged from 24.01 kDa to 25.89 kDa. Theoretical pI values ranged from 4.59 to 4.94, indicating that all *PtrCBLs* were acidic proteins. The aliphatic index varied from 85.96 to 106.76. The GRAVY of *PtrCBLs* ranged from  $-0.007$  to  $-0.305$ , suggesting their hydrophilic nature. More than half of the *PtrCBL* genes (*PtrCBL3*, 4, 7, 8, 9, 10, 11, and 13) demonstrated an instability index greater than 40, indicating potential instability and susceptibility to changes in physical, chemical properties, and biological functions. Additionally, *PtrCBL4* and *PtrCBL8* each contained one transmembrane domain. Predicting the subcellular localization of the *PtrCBL* proteins contributes to understanding their molecular functions. The analysis revealed that almost all *PtrCBL* genes were localized to the cell membrane, except for *PtrCBL6*, which was exclusively found in the cytoplasm. This unique localization suggests that *PtrCBL6* may perform specialized protein functions. Detailed information on *PtrCBLs* is presented in Table 1.

**Table 1.** Characteristic analysis of 13 *PtrCBLs* in *P. trichocarpa*.

Gene Name	Gene ID	Chromosome	Protein Length (aa)	Molecular Weight (kDa)	Theoretical pI	Instability Index	Aliphatic Index	Grand Average of Hydropathicity (GRAVY)	Transmembrane Domain	Predicted Localizations
<i>PtrCBL1</i>	Potri.001G090200	Chr01:7135427..7139480 forward	216	24,588.92	4.64	38.27	91.16	−0.221	0	Cell membrane
<i>PtrCBL2</i>	Potri.001G150200	Chr01:12540135..12545031 reverse	213	24,340.72	4.65	31.99	88.73	−0.131	0	Cell membrane
<i>PtrCBL3</i>	Potri.001G371700	Chr01:38923870..38928842 forward	223	25,672.27	4.8	42.63	95.74	−0.203	0	Cell membrane
<i>PtrCBL4</i>	Potri.003G037800	Chr03:4115827..4119014 forward	244	27,826.1	4.93	41.48	106.76	−0.007	1	Cell membrane
<i>PtrCBL5</i>	Potri.003G084200	Chr03:11086170..11091011 forward	213	24,393.73	4.7	32.07	89.67	−0.158	0	Cell membrane
<i>PtrCBL6</i>	Potri.003G141400	Chr03:15725522..15727978 reverse	226	25,727.34	4.59	36.48	94.12	−0.130	0	Cytoplasm
<i>PtrCBL7</i>	Potri.006G002900	Chr06:233213..238614 reverse	226	25,887.34	4.74	43.90	89.34	−0.290	0	Cell membrane
<i>PtrCBL8</i>	Potri.006G230200	Chr06:23364198..23366967 reverse	254	29,236.43	4.85	42.37	97.56	−0.135	1	Cell membrane
<i>PtrCBL9</i>	Potri.011G094900	Chr11:12236074..12240696 forward	222	25,803.36	4.77	44.55	90.45	−0.239	0	Cell membrane
<i>PtrCBL10</i>	Potri.012G015100	Chr12:1770445..1773882 reverse	213	24,498.86	4.78	45.93	93.29	−0.274	0	Cell membrane
<i>PtrCBL11</i>	Potri.015G013100	Chr15:845065..849858 forward	213	24,453.94	4.94	41.35	91.03	−0.305	0	Cell membrane
<i>PtrCBL12</i>	Potri.015G013200	Chr15:851384..855678 forward	213	24,009.40	4.69	39.05	85.96	−0.131	0	Cell membrane
<i>PtrCBL13</i>	Potri.016G003500	Chr16:176382..181897 reverse	226	25,894.42	4.70	40.10	91.90	−0.247	0	Cell membrane

### 3.2. Chromosome Localization and KaKs Calculation

Based on the genome annotation information of *P. trichocarpa*, the 13 *PtrCBL* genes were distributed across seven distinct chromosomes. Three *PtrCBL* genes were located on each of Chromosome 1 and Chromosome 3. Two *PtrCBL*s were positioned on each of Chromosome 6 and Chromosome 12. *PtrCBL9* was situated on Chromosome 11, *PtrCBL10* on Chromosome 12, and *PtrCBL13* on Chromosome 16 (Figure 1).

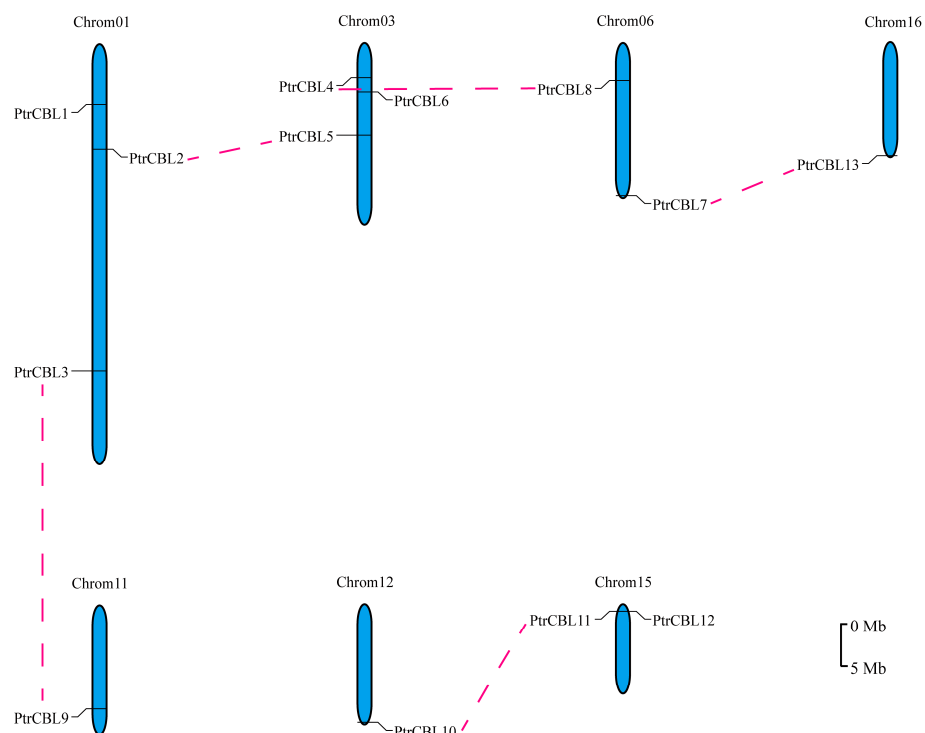


**Figure 1.** The chromosome locations and segmental paralogous pairs of *PtrCBL*s.

To analyze the selection pressures endured by the *PtrCBL* genes, we calculated the non-synonymous substitution rate ( $K_a$ ), the synonymous substitution rate ( $K_s$ ), and the  $K_a/K_s$  ratio for five *PtrCBL* gene pairs. We used the formula  $T = T = K_s/2 \times 6.1 \times 10^{-9}$  Mya to calculate the time ( $T$ ) of the duplication events [37]. The results showed that, except for *PtrCBL4-PtrCBL8*, for which no values could be calculated, the  $K_a/K_s$  ratios of the other four gene pairs ranged from 0.0751 to 0.2050, indicating that the *PtrCBL* genes have undergone purifying selection. The formation times of these segmental duplication gene pairs were approximately 4.97 to 6.81 Mya (Table 2). Taken together, these results suggest that the *PtrCBL* genes have exhibited a conservative evolutionary trend during the evolutionary process.

**Table 2.** Estimation of the age of duplicated *PtrCBL*s.

Gene Pairs	$K_a$	$K_s$	$K_a/K_s$	Date (MY)	Duplication Type
<i>PtrCBL2-PtrCBL5</i>	0.021	0.2249	0.0933	6.81	Purifying selection
<i>PtrCBL3-PtrCBL3</i>	0.01536	0.2044	0.0751	6.19	Purifying selection
<i>PtrCBL4-PtrCBL8</i>	0.2293	NaN	NaN	NaN	NaN
<i>PtrCBL7-PtrCBL13</i>	0.0247	0.1643	0.1502	4.97	Purifying selection
<i>PtrCBL10-PtrCBL11</i>	0.0337	0.1645	0.205	4.98	Purifying selection

### 3.3. Phylogenetic Analysis

The analysis of homologous genes provides a foundation for exploring gene functions. The phylogenetic analysis revealed that the *PtrCBL* genes could be categorized into five subfamilies (Group I–V). Each subgroup exhibited uneven distribution in terms of member count. Group I contained the largest number of *PtrCBL* members (*PtrCBL1, 6, 10, 11*, and

12). *PtrCBL4* and 8 were located in Group II, while *PtrCBL2* and 5 were found in Group III. Group IV comprised two *PtrCBL* genes, including *PtrCBL3* and 9. Both *PtrCBL7* and 13 were grouped in Group V (Figure 2). It is well established that proteins with closer genetic relationships often exhibit similar or closely related biological functions. Furthermore, the majority of *PtrCBL* proteins clustered with the *CBL* proteins in *Glycine max*. This clustering pattern suggests that the *PtrCBL* proteins have a closer genetic relationship with their homologous counterparts in *Glycine max* compared to those in *Arabidopsis thaliana*.

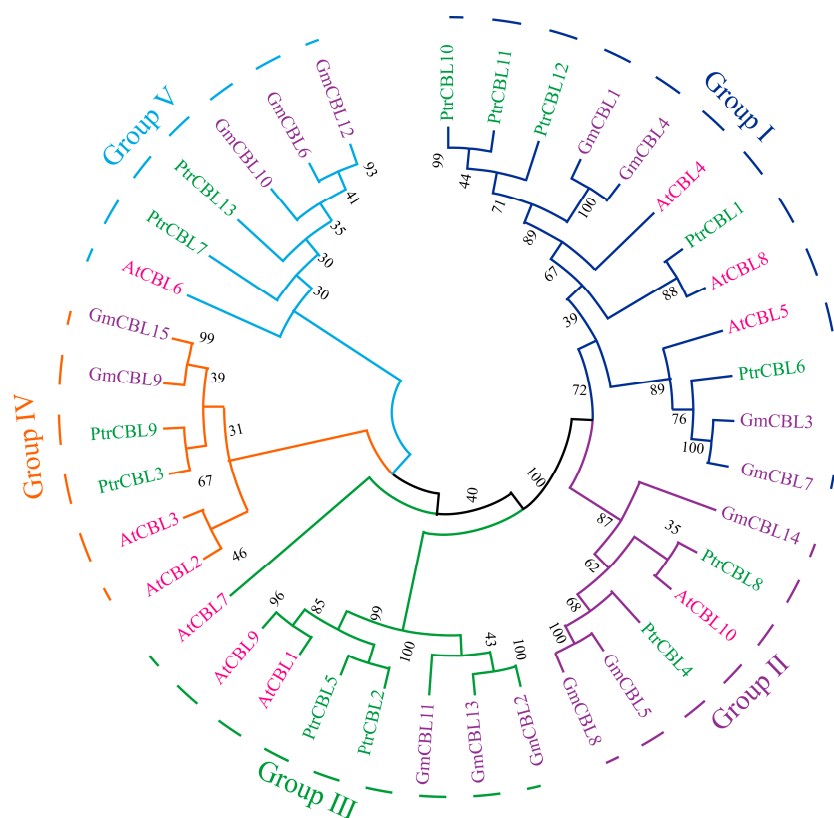


**Figure 2.** Phylogenetic tree of the *CBLs* in *Populus trichocarpa*, *Arabidopsis thaliana*, and *Glycine max*. Fonts in different colors represent different species.

### 3.4. Gene Structure and Conserved Motifs

Analysis of gene structure can elucidate conserved characteristics and potential biological functions. Multiple sequence alignment revealed that all *PtrCBL* proteins contained EF-hand domains 1–4. Twelve *PtrCBL* proteins exhibited the FPSF motif at the C-terminus, with the exception of *PtrCBL6*. Notably, the N-terminal MGCXXSK/T motif, recognized as the myristoylation domain, is a specialized *CBL* protein domain [38]. This domain was present only in *PtrCBL2*, 5, 10, 11, and 12 (Figure 3).

Analysis of gene structure revealed similarities in length, exon count, and intron number among members within the same subfamily (Figure 4A). Notably, all *PtrCBL* members, except *PtrCBL8*, contained seven introns, indicating conservation in the evolution of *PtrCBLs* (Figure 4B). Furthermore, the number of introns often correlates with gene expression level, suggesting these genes may be highly expressed in cells [39]. Conserved motifs shared by most members of a gene family typically play crucial roles in the family's function or structure. Analysis of conserved motifs demonstrated that all *PtrCBLs* contained motifs 1, 2, 3, and 5, which are characteristic of conserved EF-hand domain structures. Motif 10 was unique to *PtrCBL4* and *PtrCBL8*, while *PtrCBL6* lacked motif 7. Most *PtrCBL* proteins possessed seven motifs, although the specific types varied. *PtrCBL7* and *PtrCBL13*

exhibited nine conserved motifs (Figure 4C). Detailed sequences of ten motifs are presented in Supplementary Table S4.

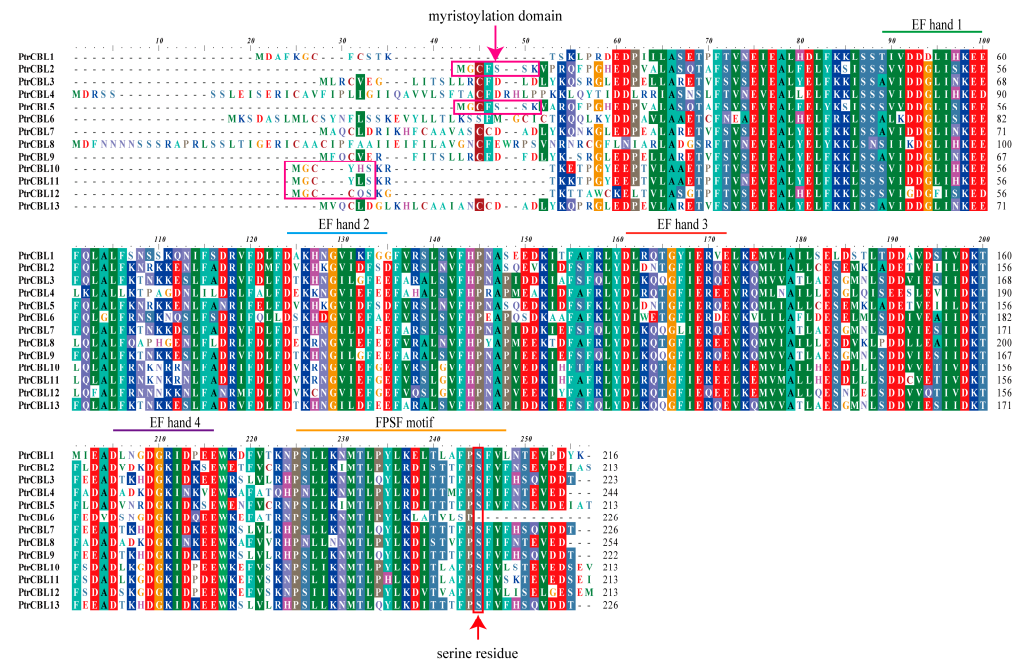


**Figure 3.** The multiple sequence alignment of *PtrCBLs* in *P. trichocarpa*. The different EF-hand domains are marked by different colored lines. The magenta frame tagged the myristoylation domain.

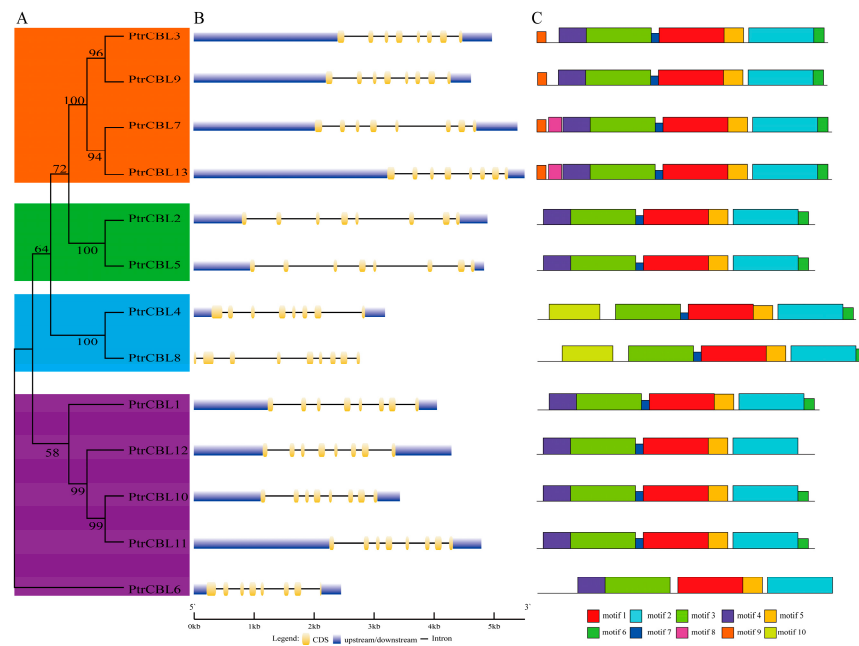


**Figure 4.** Gene structure of *PtrCBLs*. (A) Phylogenetic tree within *PtrCBLs* in *P. trichocarpa*. The different background color represents the subgroup. (B) The exon–intron structure analysis of *PtrCBLs*. (C) The conserved motifs in *PtrCBL* proteins. MEME website was used to identify the conserved motifs. Modules in different colors represent different motifs.

### 3.5. Promoter *cis*-Element Analysis

Promoter *cis*-acting elements, crucial binding regions for transcription initiation factors, play a significant role in regulating gene expression [40]. To further analyze the potential biological functions of the *PtrCBLs*, we examined their promoter *cis*-acting elements using the PlantCARE website. We identified 10 distinct types of promoter *cis*-acting elements in the



*PtrCBLs* promoter region, including abscisic acid-responsive elements (ABRE), methyl jasmonate (MeJA)-responsive elements (CGTCA/TGACG), salicylic acid-responsive elements (TCA), auxin-responsive elements (TGA), drought-inducible elements (MBS), gibberellin-responsive elements (GARE/TATC-box/P-box), and low-temperature-responsive elements (LTR). Detailed cis-acting element information is provided in Supplementary Table S5. The distribution of these cis-acting elements varied considerably among *PtrCBL* promoters. For example, *PtrCBL6* contained the largest variety of cis-acting elements, while *PtrCBL11* contained only one LTR. With the exception of *PtrCBL7*, 9, and 11, all *PtrCBLs* contained varying numbers of ABRE elements, with *PtrCBL2* having the highest number. Additionally, only *PtrCBL3* and *PtrCBL4* contained one TGA element and TATC-box, respectively (Figure 5).

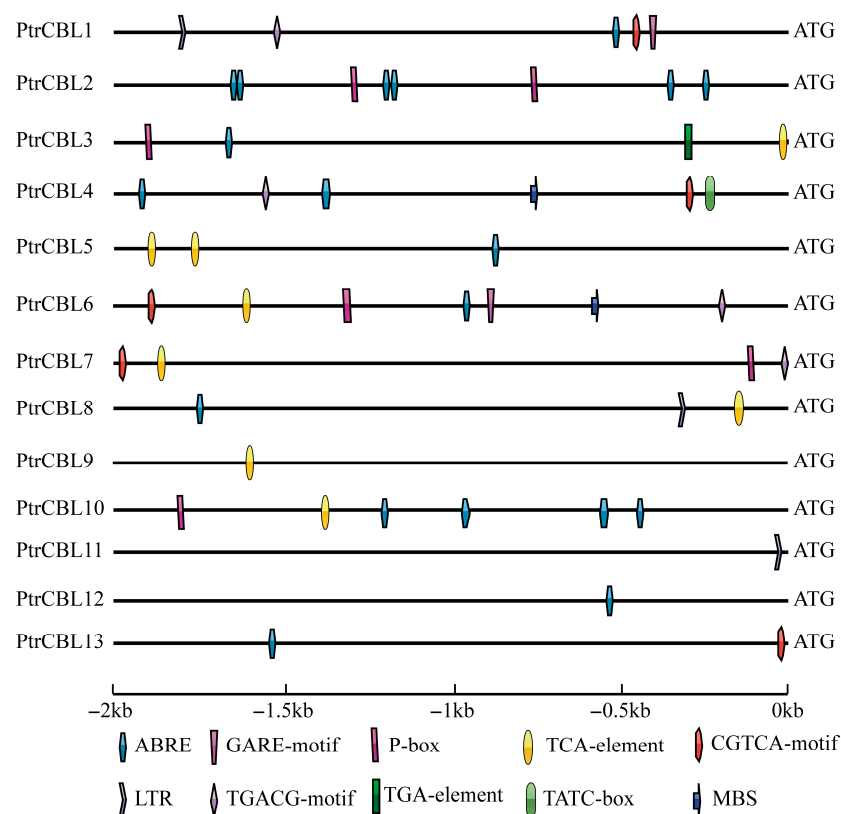


**Figure 5.** Distribution of cis-elements in *PtrCBL* promoter regions. Different shapes represent different types of cis-elements.

### 3.6. Protein Tertiary Structure

The tertiary structure of *PtrCBL* proteins was analyzed using Swiss-Model online platform. The results revealed diverse protein tertiary structures among the 13 *PtrCBL* members. Notable differences in *PtrCBL* tertiary structures were observed, likely related to structural elements, including  $\alpha$ -helices,  $\beta$ -sheets, and random coils. The similarities and differences in tertiary structures may explain the functional similarities or differences exhibited among proteins. Importantly, homologous gene pairs such as *PtrCBL2*-*PtrCBL5*, *PtrCBL3*-*PtrCBL9*, *PtrCBL4*-*PtrCBL8*, *PtrCBL7*-*PtrCBL13*, and *PtrCBL10*-*PtrCBL11* displayed highly similar protein tertiary structures, suggesting functional redundancy among these pairs (Figure 6).

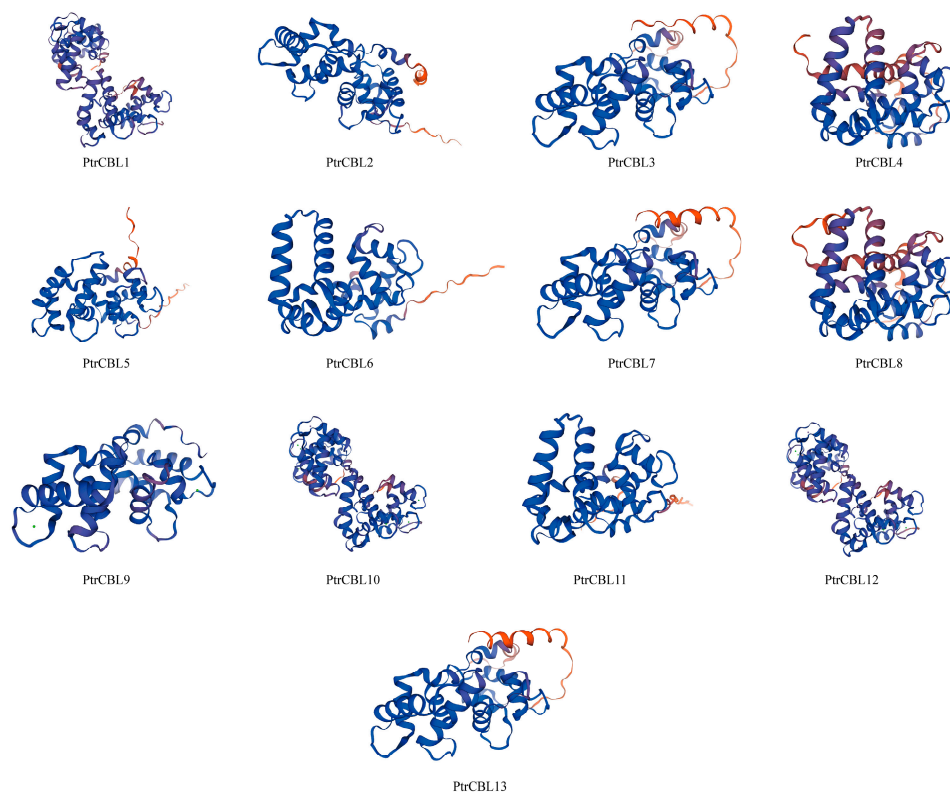


**Figure 6.** The protein tertiary structure of PtrCBLs.

### 3.7. Protein Interaction Network

We utilized the STRING website to predict potential interacting proteins for PtrCBLs. The analysis revealed that all PtrCBL proteins possessed interacting protein networks, suggesting that PtrCBL members can interact with other proteins in response to plant hormone treatments and environmental stresses, as well as participate in growth and development processes in *P. trichocarpa*. Furthermore, PtrCBL1, 3, 4, 6, 8, 9, 10, and 13 exhibited similar interacting proteins, indicating the presence of conserved interaction domains within the PtrCBL protein (Figure 7). Previous research has demonstrated that CBL proteins can specifically bind to CBL-interacting protein kinases (CIPK) to form CBL-CIPK protein complexes. These complexes participate in the  $\text{Ca}^{2+}$  signal transduction pathway, enabling plants to respond to various internal and external signals [41]. Our results indicated that all PtrCBL proteins interact with different CIPK proteins, suggesting that this interaction exists in *P. trichocarpa* to facilitate growth, development, and abiotic stress resistance.

### 3.8. Prediction in Phosphorylation Sites

Prior research has demonstrated that CBL proteins can undergo phosphorylation by CIPK proteins [42]. Consequently, we predicted potential phosphorylation sites in PtrCBL proteins, focusing primarily on serine, threonine, and tyrosine sites. As illustrated in Figure 8, all PtrCBL proteins contained serine phosphorylation sites, albeit in varying numbers. For instance, PtrCBL2 and PtrCBL12 exhibited fifteen serine sites each, followed by PtrCBL3, 5, and 9, which possessed fourteen serine sites. PtrCBL8 displayed the fewest serine sites, with only eight. PtrCBL10 and PtrCBL12 contained the highest number of threonine sites. The PtrCBL protein with the least serine sites was PtrCBL2, containing only three. With the exception of PtrCBL2 and PtrCBL5, all PtrCBL proteins contained tyrosine sites, though most PtrCBL proteins only exhibited one to three tyrosine sites.

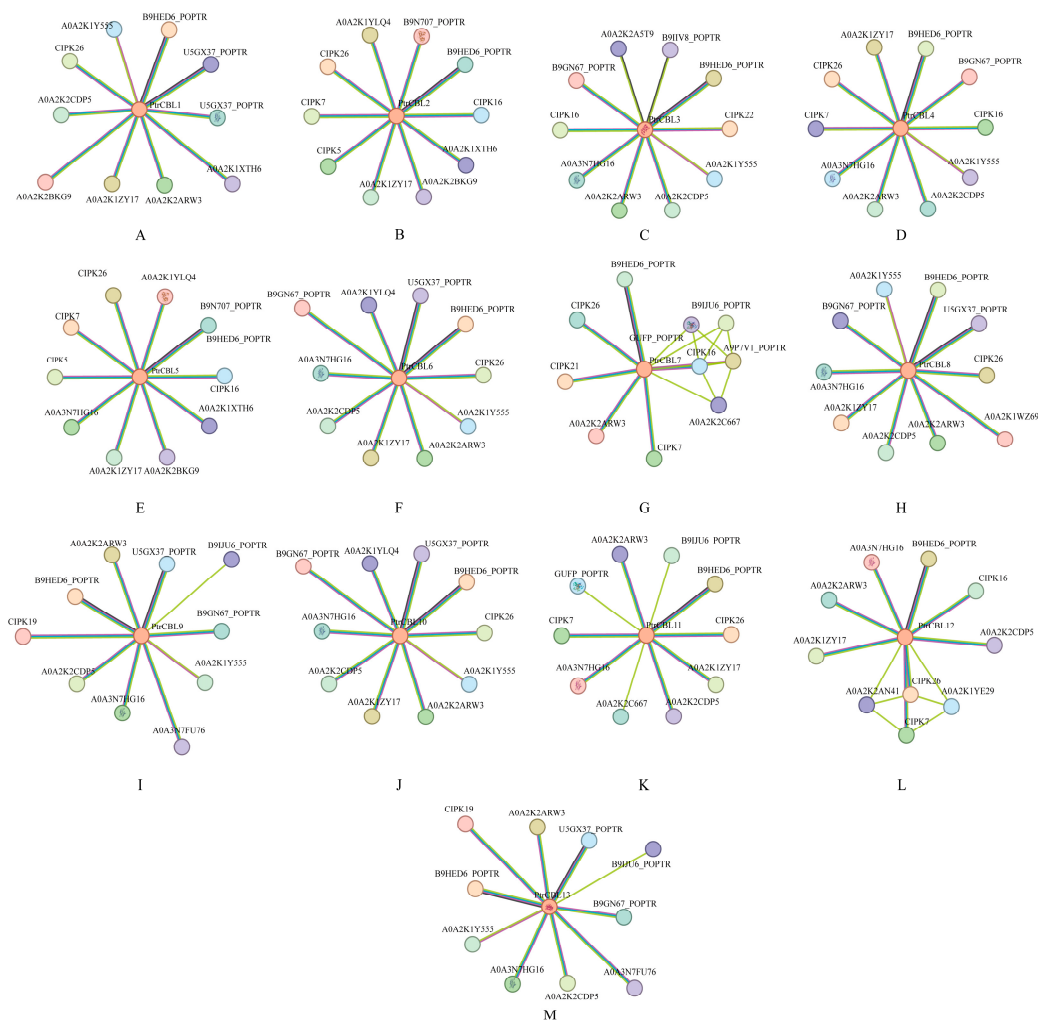


**Figure 7.** The predicted protein interaction networks of PtrCBL proteins. (A–M) represents the interaction network of each PtrCBL protein.

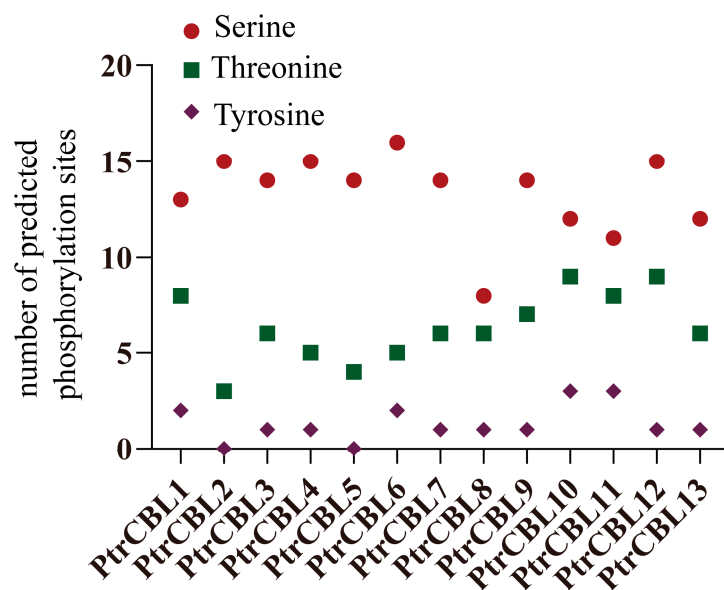


**Figure 8.** The predicted phosphorylation sites in the PtrCBL amino acid sequence. Different colored modules represent serine, threonine, and tyrosine sites, respectively.

### 3.9. RNA-Seq and Expression Heatmap

Previous research has documented that halophytes typically exhibit specific morphological and anatomical adaptations in response to salt stress. These adaptations primarily include alterations in stomatal size, development of a multi-layered epidermis, thickening of the cuticle, early lignification, inhibited differentiation, and changes in the diameter and number of xylem vessels [43]. In this study, leaves from *P. simonii* × *P. nigra* subjected to low and high concentrations of alkaline stress were used as plant materials, with *P. trichocarpa* serving as the reference genome for transcriptome sequencing analysis. The analysis of transcriptome data revealed a total of 10,657 differentially expressed genes (DEGs), comprising 6613 down-regulated and 4044 up-regulated genes (Figure 9A).



**Figure 9.** Differentially expressed genes (DEGs) in the leaves of *P. simonii* × *P. nigra* under alkaline stress. (A) DEGs statistics of RNA-seq in *P. simonii* × *P. nigra* under alkaline stress. Different colored

bars represent the number of up-regulated, down-regulated, and total DEGs in the transcriptome. (B) Heatmap of the expression profiles of 13 *PsnCBL* genes under alkaline stress using RNA-seq data. The different colored boxes indicate different  $\log_2(\text{FPKM})$  values, with expression gradually increasing from blue to yellow to red over time. (C) The biological process at 7 d under low-concentration alkaline stress. (D) The biological process at 7 d under high-concentration alkaline stress. (E) The biological process at 14 d under low-concentration alkaline stress. (F) The biological process at 14 d under high-concentration alkaline stress.

To investigate the functions of *PsnCBLs* under low- and high-concentration alkaline stress in poplar, we analyzed gene expression levels using transcriptome data. Notably, *PtrCBL1* showed negligible count values. A heatmap of expression patterns was constructed based on  $\log_2(\text{FPKM})$  values. As depicted in Figure 9B, the majority of *PsnCBL* genes exhibited significant up-regulation or down-regulation at 7 or 14 days under low- or high-concentration alkaline stress, suggesting *PsnCBLs*' involvement in the alkaline stress response in *P. simonii* × *P. nigra*. Specifically, *PsnCBL2* was significantly up-regulated under low-concentration alkaline stress conditions at 7 d, while *PsnCBL4*, 5, and 6 were significantly down-regulated. However, after 14 d of low-concentration alkaline stress, *PsnCBL3*, 4, 6, 7, 8, 10, and 13 were significantly up-regulated, and *PsnCBL5* was significantly down-regulated, with other genes showing no significant change. Under high-concentration alkaline stress at 7 d, the expression levels of *PsnCBL4*, 8, and 13 were significantly up-regulated, while four genes (*PsnCBL2*, 5, 9, and 10) were significantly down-regulated, and four genes showed no significant difference in expression levels. At 14 days of high-concentration alkaline stress, *PsnCBL2*, 3, 5, 8, and 12 were significantly up-regulated, two genes were down-regulated, and eight genes showed no significant change. Notably, *PsnCBL3* and *PsnCBL8* were significantly up-regulated at all three time points under both low- and high-concentration alkaline stress, indicating their important roles in the response to alkaline stress in poplar. The transcriptome data for *PsnCBLs* is provided in Supplementary Table S6.

Following our transcriptome analysis, we performed Gene Ontology (GO) enrichment based on the identified DEGs. The results revealed that multiple biological processes are involved in the response to alkaline stress in *P. simonii* × *P. nigra*. These processes include carbohydrate metabolic process, protein phosphorylation, iron ion transport, iron ion homeostasis, and transmembrane transport (Figure 9C–F). Notably, for high alkaline stress at 7 d and both low and high alkaline stresses at 14 d, the DEGs were predominantly enriched in the biological process of protein phosphorylation. This finding suggests that *PsnCBL* proteins may contribute to alkaline stress through the phosphorylation pathway.

### 3.10. Expression Pattern of *Populus simonii* × *Populus nigra* Under Alkaline Stress

To validate the transcriptome data reliability, RT-qPCR was employed to access the expression of nine *PsnCBLs* (*PsnCBL2*, 3, 4, 5, 6, 8, 10, 12, and 13) with relatively high FPKM values in the transcriptome data. The evaluation revealed that the expression trends of these genes were generally consistent with the transcript abundance changes in the transcriptome data, confirming its reliability (Figure 10a,b). Further analysis under low-concentration alkaline stress showed significant up-regulation of *PsnCBL3* and *PsnCBL15* at 7 d and 14 d. *PsnCBL4* and *PsnCBL6* were markedly down-regulated at 7 d and dramatically up-regulated at 14 d. *PsnCBL2* exhibited significant up-regulation at 7 d and slight up-regulation at 14 d. *PsnCBL5* was significantly down-regulated at 7 d and slightly up-regulated at 14 d. *PsnCBL8* and *PsnCBL10* showed significant up-regulation at 14 d, while *PsnCBL12* was slightly up-regulated at both 7 d and 14 d. Under high-concentration alkaline stress, only *PsnCBL8* was consistently up-regulated at 7 d and 14 d. *PsnCBL2* and *PsnCBL5* were significantly down-regulated at 7 d and remarkably up-regulated at 14 d. *PsnCBL4* and



*PsnCBL13* were significantly up-regulated at 7 d, with *PsnCBL4* slightly down-regulated and *PsnCBL13* slightly up-regulated at 14 d. *PsnCBL3* and *PsnCBL12* showed significant up-regulation at 14 d, while *PsnCBL10* was slightly down-regulated at both 7 d and 14 d (Figure 10a,b).

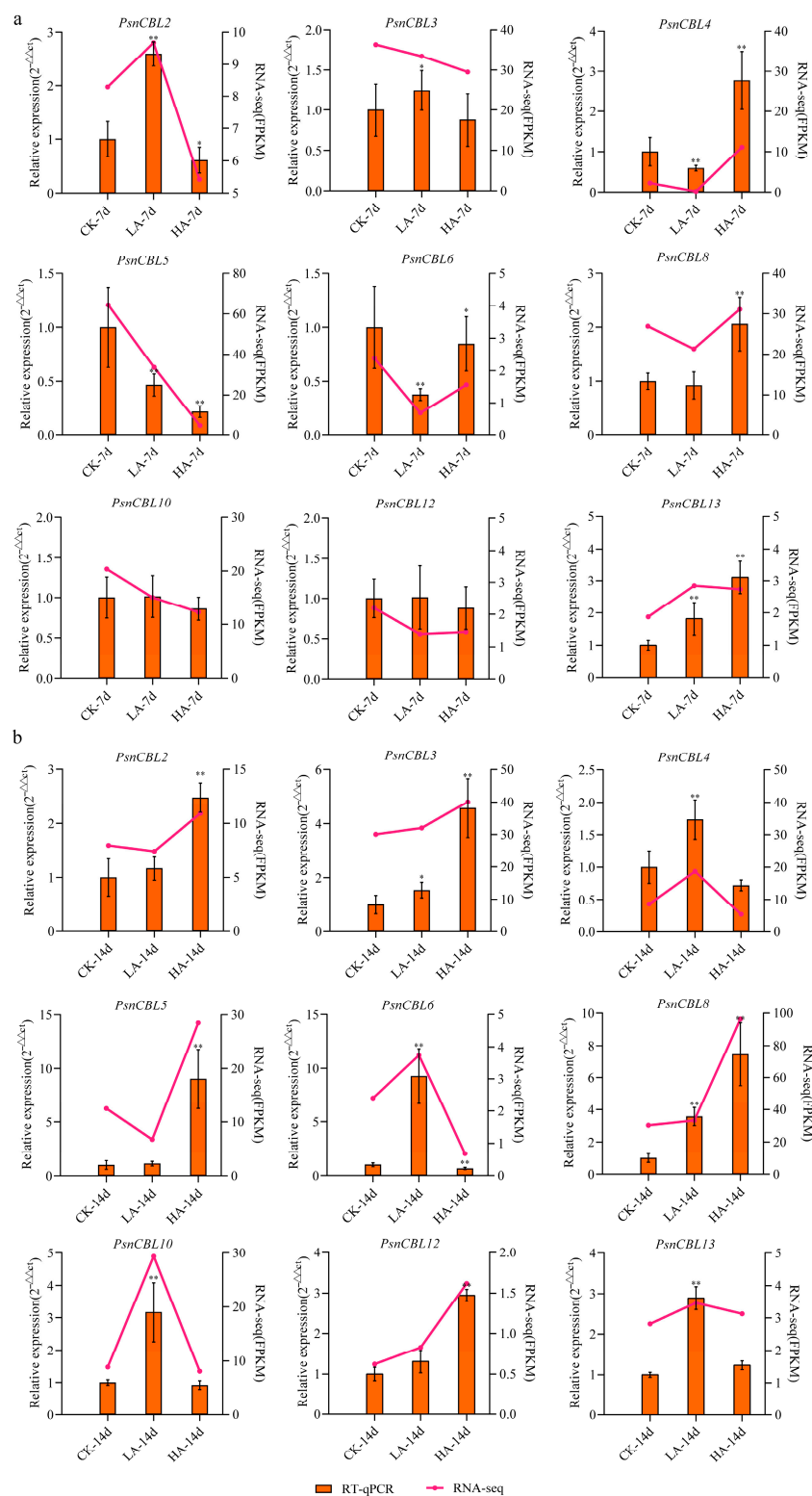


**Figure 10.** Validation of the expression data of nine *PsnCBL* genes from RNA-seq by RT-qPCR. The data are expressed as the mean  $\pm$  standard deviation of the three biological replicates. An asterisk (\*) represents a significant difference ( $p < 0.05$ ), and double asterisks (\*\*) represent an extremely

significant difference ( $p < 0.01$ ). (a) Expression analysis of *PsnCBLs* between RNA-seq and RT-qPCR at 7 d under different concentrations of alkaline stress. (b) Expression analysis of *PsnCBLs* between RNA-seq and RT-qPCR at 14 d under different concentrations of alkaline stress.

## 4. Discussion

### 4.1. The CBL Family Genes in *Populus trichocarpa*

Calcineurin B-like proteins (CBLs), which function as plant-specific calcium sensors, are most similar to calcineurin B and neuronal calcium sensor proteins. They have been recognized as crucial components in diverse  $\text{Ca}^{2+}$ -dependent processes in plants [44]. CBLs play a significant role in influencing biological and abiotic stress processes through  $\text{Ca}^{2+}$ -related pathways [45]. The functions of CBL genes have been identified in various plants, including *Arabidopsis thaliana* [2], *Oryza sativa* [10], *Vitis vinifera* [13], and *Saccharum officinarum* [46]. However, until now, there has been limited bioinformatics analysis information on CBL genes in poplar. In this study, 13 *PtrCBL* genes were identified in the *P. trichocarpa* genome, all containing four EF-hand motifs. Multiple sequence alignment analysis, as shown in Figure 3, revealed that all *PtrCBLs* except *PtrCBL6* contain the FPSF motif at the C-terminus, indicating that *PtrCBL6* may be phosphorylated by CIPK through an alternative phosphorylation site, warranting further experimental verification. Previous studies have reported that the serine site in the FPSF motif can be phosphorylated by CIPK [47]. For instance, AtCIPK23 can phosphorylate the C-terminal FPSF motif within AtCBL1 and AtCBL9, thereby enhancing the interaction between CBL and CIPK proteins [8]. It is noteworthy that the 226th Ser of *PtrCBL4* and *PtrCBL8* was replaced with Asn in the FPSF motif. The same results were also found in *Arabidopsis*, in which the Ser site changed to Thr [2]. This diverges from the absolute conservation of the Ser site within the PFPF motif of *OsCBLs* and *VvCBLs* [10,13]. Our subcellular localization prediction results showed that 12 *PtrCBL* proteins were located on the cell membrane, while only *PtrCBL6* was positioned in the cytoplasm (Table 1). However, *PtrCBL1*–*PtrCBL6*, which serve as homologous genes, were located in the cytoplasm, indicating that homologous genes or conserved domains do not necessarily share the same subcellular localization. This also suggests that homologous genes may exhibit differences in gene functions and signal transduction.

Multiple studies have demonstrated that the domains within genes play a crucial role in determining gene functions [48]. All *PtrCBL* proteins contain four EF-hand domains, with highly conserved connection intervals between each domain. Specifically, there are 22 amino acids between EF1 and EF2, 25 amino acids between EF2 and EF3, and 32 amino acids between EF3 and EF4 (Figure 3). These findings align closely with the CBL protein structures observed in *Arabidopsis thaliana* and *Saccharum officinarum* [2,13]. Four *PtrCBL* proteins (*PtrCBL2*, 5, 11, and 12) possess myristoylation sites (MGXXS/T) at the N-terminus (Figure 3). N-terminal myristoylation facilitates protein attachment to membranes and enhances protein–protein interactions [49]. Furthermore, previous research has shown that myristoylation sites contribute to improved salt stress resistance [50], suggesting that *PtrCBL2*, 5, 11, and 12 may play significant roles in the poplar's response to salt stress.

### 4.2. Promoter *cis*-Acting Elements of *PtrCBLs*

Previous research indicates that promoter *cis*-elements play critical roles in transcriptional regulation when plants are subjected to biotic and abiotic stresses. These elements include ABRE, MeJA-responsive elements (CGTCA), gibberellin-responsive elements (GARE-motif), auxin-responsive elements (TGA-element), P-box, LTR, salicylic acid-responsive elements (TCA-element), TC-rich repeats, TGACG motif, and drought-inducible elements (MBS *cis*-element). Analysis of *PtrCBL* promoter *cis*-acting elements reveals that each *PtrCBL* contains at least one abiotic-related stress or hormone-related responsive *cis*-acting

element, suggesting that PtrCBLs play significant roles in responding to abiotic stress and hormone signals in poplar. All PtrCBLs, except PtrCBL9 and PtrCBL12, contain ABRE (Figure 5). The response mechanisms of CBL genes to ABA-mediated abiotic stress have been studied in *Arabidopsis thaliana* [51]. This phenomenon suggests that PtrCBL genes participate in the ABA-mediated signaling pathway to respond to abiotic stress.

#### 4.3. The Predicted Protein Interaction Network of PtrCBLs

In plants, CBL proteins interact with CIPK proteins and play a crucial role in the stress response mechanism to external stimuli [52]. Protein interaction networks are significant for interpreting various  $\text{Ca}^{2+}$  signals to adapt to changing environments [53]. The predicted protein interaction networks demonstrated that all PtrCBL proteins interacted with CIPK proteins (as shown in Figure 6). *PtrCBL2* and *PtrCBL5* were homologous genes (as shown in Figure 4A). Our results indicated that both *PtrCBL2* and *PtrCBL5* interacted with PtrCIPK5, 7, 16, and 26, suggesting functional redundancy of homologous genes. Previous studies have shown that in the reactive oxygen species (ROS) pathway, AtCBL1 and AtCBL9 interact with AtCIPK26 and play a regulatory role in the NADPH oxidase RbohF in *Arabidopsis* [54]. *PtrCBL2* and *PtrCBL5* serve as homologous genes of AtCBL1 and AtCBL9 in *Arabidopsis*. Additionally, *PtrCBL2* and *PtrCBL5*, which contain myristoylation sites at the C-terminus, can promote protein attachment to membranes and protein–protein interactions [49]. Increasing evidence has also shown that the homologous genes of *PtrCBL2* and *PtrCBL5* in *Populus euphratica*, PeCBL1, interact with PeCIPK24, PeCIPK25, and PeCIPK26 and regulate the homeostasis of  $\text{Na}^+$  and  $\text{K}^+$  in *Populus euphratica* [55]. This indicates that the interaction between *PtrCBL2* and *PtrCBL5* with CIPK proteins is of great significance in the NADPH oxidase pathway and in regulating  $\text{Na}^+$  and  $\text{K}^+$  homeostasis in poplar.

#### 4.4. Expression Patterns and RNA-Seq Analysis of *PsbCBLs* Under Alkaline Stress

CBL proteins play a crucial role in metabolic and growth-related activities during plant life cycles [15]. While most studies on CBL gene functions have primarily focused on salt stress, drought, and hormone responses [56–58], there has been limited research on the expression patterns of *CBLs* under alkaline stress in poplar. Salinity and alkalinity are major abiotic stresses that impede growth and development in poplar [23]. Previous research has indicated that alkaline salts have a significantly stronger detrimental effect on plants compared to neutral salts. In saline-alkali soil containing bicarbonate ions ( $\text{HCO}_3^-$ ), plants are subjected to the dual damaging effects of both salt and alkaline stress [59]. Consequently, soda alkaline was selected for alkaline stress treatment in *P. simonii* × *P. nigra*. Transcriptome data analysis revealed that the number of DEGs under high-concentration alkaline stress was generally greater than that under low-concentration alkaline stress, indicating that the high-concentration alkaline stress treatment caused severe damage to *P. simonii* × *P. nigra*, which aligns with previous findings [23]. The combined analysis of RT-qPCR and transcriptome data demonstrated that nine *PsnCBL* genes were induced under different concentrations of alkaline stress at various time points (Figure 10a,b), indicating that CBL genes play a significant role in response to alkaline stress in poplar. GO analysis showed that protein phosphorylation had the largest number of DEGs in biological processes under both low- and high-concentration alkaline stress (Figure 9C–F). This phenomenon indicates that CBL-mediated phosphorylation may trigger responses in multiple biological processes to cope with external alkaline stress in poplar. Previous research has shown that when plants are exposed to high  $\text{Na}^+$  environments, it leads to an imbalance in cellular ion concentrations and causes various negative impacts, such as impairment of photosynthesis and disruption of enzyme activities. In such situations, the

intracellular  $\text{Ca}^{2+}$  concentration increases, triggering the activation of CBL proteins. These activated proteins bind to CIPK proteins and further activate downstream targets involved in regulating ion transport and homeostasis. Through this process, the CBL-CIPK signaling pathway can help prevent the accumulation of  $\text{Na}^+$  [60]. The extensive data obtained from this research, specifically regarding the connection between CBL genes and alkaline stress in poplar, constitutes a robust basis for future experiments.

## 5. Conclusions

Overall, 13 CBL genes were identified in the *P. trichocarpa* genome for the first time. Through multiple sequence alignment, chromosome localization, phylogenetic relationships, promoter *cis*-acting elements, phosphorylation site prediction, and protein interaction networks, a systematic analysis was conducted on the 13 *PtrCBL* genes. RNA-seq and RT-qPCR techniques were used to analyze the expression patterns and functions of the CBL family in *P. simonii* × *P. nigra* under alkaline stress. Our research provides a basis for the subsequent functional identification of the CBL genes and the study of their response to alkaline stress in poplar. More experiments will be conducted to verify the function of specific CBL genes under alkaline stress in poplar in future research.

**Supplementary Materials:** The following supporting information can be downloaded at: <https://www.mdpi.com/article/10.3390/f16020200/s1>, Table S1: The AtCBL gene ID, protein sequences and sequence similarity between *P. trichocarpa* and *Arabidopsis*; Table S2 and Figure S1: Results of quality check of RNA; Table S3: The primers used in RT-qPCR; Table S4: The sequence consensus of *PtrCBLs* conserved motifs; Table S5: The *cis*-acting element information; Table S6: The detailed *PsnCBL* information of transcriptome in *Populus simonii* × *Populus nigra* under alkaline stress.

**Author Contributions:** Conceptualization, H.W., J.Y. and X.L.; methodology, J.W. and X.L.; software, H.W.; validation, Z.J. and X.L.; formal analysis, H.W.; investigation, H.W.; resources, J.W.; data curation, J.W.; writing—original draft preparation, H.W.; writing—review and editing, J.Y. and X.L.; visualization, H.W.; supervision, Z.J.; project administration, X.L.; funding acquisition, H.W. and X.L. All authors have read and agreed to the published version of the manuscript.

**Funding:** This research was funded by the Natural Science Foundation of Jilin Province, grant number YDZJ202201ZYTS454, and the Doctor startup fund of Jilin Agricultural Science and Technology University, grant number XJ2021001106.

**Data Availability Statement:** RNA-Seq data under alkaline stress can be found under accession number: GSE285903.

**Conflicts of Interest:** The authors declare no conflicts of interest.

## References

1. Xiong, L.; Schumaker, K.S.; Zhu, J.K. Cell signaling during cold, drought, and salt stress. *Plant Cell* **2002**, *14* (Suppl. 1), S165–S183. [[CrossRef](#)] [[PubMed](#)]
2. Kolukisaoglu, U.; Weinl, S.; Blazevic, D.; Batistic, O.; Kudla, J. Calcium sensors and their interacting protein kinases: Genomics of the *Arabidopsis* and rice CBL-CIPK signaling networks. *Plant Physiol.* **2004**, *134*, 43–58. [[CrossRef](#)]
3. Dodd, A.N.; Kudla, J.; Sanders, D. The language of calcium signaling. *Annu. Rev. Plant Biol.* **2010**, *61*, 593–620. [[CrossRef](#)] [[PubMed](#)]
4. Tang, R.J.; Wang, C.; Li, K.; Luan, S. The CBL-CIPK calcium signaling network: Unified paradigm from 20 Years of discoveries. *Trends Plant Sci.* **2020**, *25*, 604–617. [[CrossRef](#)]
5. Jiang, Y.; Zhang, H.; Li, Y.; Chang, C.; Wang, Y.; Feng, H.; Li, R. A novel transcriptional regulator HbERF6 regulates the HbCIPK2-Coordinated pathway conferring salt tolerance in halophytic *Hordeum brevisubulatum*. *Front. Plant Sci.* **2022**, *13*, 927253. [[CrossRef](#)] [[PubMed](#)]
6. Batistic, O.; Kudla, J. Plant calcineurin B-like proteins and their interacting protein kinases. *Biochim. Biophys. Acta* **2009**, *6*, 985–992. [[CrossRef](#)] [[PubMed](#)]

7. Tang, R.J.; Liu, H.; Yang, Y.; Yang, L.; Gao, X.S.; Garcia, V.J.; Luan, S.; Zhang, H.X. Tonoplast calcium sensors CBL2 and CBL3 control plant growth and ion homeostasis through regulating V-ATPase activity in *Arabidopsis*. *Cell Res.* **2012**, *22*, 1650–1665. [[CrossRef](#)] [[PubMed](#)]
8. Hashimoto, K.; Eckert, C.; Anschutz, U.; Scholz, M.; Held, K.; Waadt, R.; Reyer, A.; Hippler, M.; Becker, D.; Kudla, J. Phosphorylation of calcineurin B-like (CBL) calcium sensor proteins by their CBL-interacting protein kinases (CIPKs) is required for full activity of CBL-CIPK complexes toward their target proteins. *J. Biol. Chem.* **2012**, *287*, 7956–7968. [[CrossRef](#)]
9. Kudla, J.; Xu, Q.; Harter, K.; Gruissem, W.; Luan, S. Genes for calcineurin B-like proteins in *Arabidopsis* are differentially regulated by stress signals. *Proc. Natl. Acad. Sci. USA* **1999**, *96*, 4718–4723. [[CrossRef](#)]
10. Kanwar, P.; Sanyal, S.K.; Tokas, I.; Yadav, A.K.; Pandey, A.; Kapoor, S.; Pandey, G.K. Comprehensive structural, interaction and expression analysis of CBL and CIPK complement during abiotic stresses and development in rice. *Cell Calcium.* **2014**, *56*, 81–95. [[CrossRef](#)]
11. Zhang, Y.; Zhou, X.; Liu, S.; Yu, A.; Yang, C.; Chen, X.; Liu, J.; Wang, A. Identification and functional analysis of tomato CIPK gene family. *Int. J. Mol. Sci.* **2019**, *21*, 110. [[CrossRef](#)] [[PubMed](#)]
12. Sun, W.; Zhang, B.; Deng, J.; Chen, L.; Ullah, A.; Yang, X. Genome-wide analysis of CBL and CIPK family genes in cotton: Conserved structures with divergent interactions and expression. *Physiol. Mol. Biol. Plants* **2021**, *27*, 359–368. [[CrossRef](#)] [[PubMed](#)]
13. Xi, Y.; Liu, J.; Dong, C.; Cheng, Z.M. The CBL and CIPK gene family in grapevine (*Vitis vinifera*): Genome-Wide analysis and expression profiles in response to various abiotic stresses. *Front. Plant Sci.* **2017**, *8*, 978. [[CrossRef](#)] [[PubMed](#)]
14. Aslam, M.; Fakher, B.; Jakada, B.H.; Zhao, L.; Cao, S.; Cheng, Y.; Qin, Y. Genome-Wide identification and expression profiling of CBL-CIPK gene family in pineapple (*Ananas comosus*) and the role of *AcCBL1* in abiotic and biotic stress response. *Biomolecules* **2019**, *9*, 293. [[CrossRef](#)]
15. Ma, X.; Li, Q.H.; Yu, Y.N.; Qiao, Y.M.; Haq, S.U.; Gong, Z.H. The CBL-CIPK pathway in plant response to stress signals. *Int. J. Mol. Sci.* **2020**, *21*, 5668. [[CrossRef](#)] [[PubMed](#)]
16. Mahs, A.; Steinhorst, L.; Han, J.P.; Shen, L.K.; Wang, Y.; Kudla, J. The calcineurin B-like Ca<sup>2+</sup> sensors CBL1 and CBL9 function in pollen germination and pollen tube growth in *Arabidopsis*. *Mol. Plant* **2013**, *6*, 1149–1162. [[CrossRef](#)]
17. D'Angelo, C.; Weinl, S.; Batistic, O.; Pandey, G.K.; Cheong, Y.H.; Schultke, S.; Albrecht, V.; Ehlert, B.; Schulz, B.; Harter, K.; et al. Alternative complex formation of the Ca-regulated protein kinase CIPK1 controls abscisic acid-dependent and independent stress responses in *Arabidopsis*. *Plant J.* **2006**, *48*, 857–872. [[CrossRef](#)] [[PubMed](#)]
18. Aslam, M.; Greaves, J.G.; Jakada, B.H.; Fakher, B.; Wang, X.; Qin, Y. *AcCIPK5*, a pineapple CBL-interacting protein kinase, confers salt, osmotic and cold stress tolerance in transgenic *Arabidopsis*. *Plant Sci.* **2022**, *320*, 111284. [[CrossRef](#)] [[PubMed](#)]
19. Jiao, F.; Zhang, D.; Chen, Y.; Wu, J. Genome-Wide identification of members of the soybean CBL gene family and characterization of the functional role of *GmCBL1* in responses to saline and alkaline stress. *Plants* **2024**, *13*, 1304. [[CrossRef](#)]
20. Wu, S.J.; Ding, L.; Zhu, J.K. *SOS1*, a genetic locus essential for salt tolerance and potassium acquisition. *Plant Cell* **1996**, *8*, 617–627. [[CrossRef](#)] [[PubMed](#)]
21. Fuglsang, A.T.; Guo, Y.; Cuin, T.A.; Qiu, Q.; Song, C.; Kristiansen, K.A.; Bych, K.; Schulz, A.; Shabala, S.; Schumaker, K.S.; et al. *Arabidopsis* protein kinase *PKS5* inhibits the plasma membrane H<sup>+</sup>-ATPase by preventing interaction with 14-3-3 protein. *Plant Cell* **2007**, *19*, 1617–1634. [[CrossRef](#)] [[PubMed](#)]
22. Ji, H.; Pardo, J.M.; Batelli, G.; Van Oosten, M.J.; Bressan, R.A.; Li, X. The Salt Overly Sensitive (SOS) pathway: Established and emerging roles. *Mol. Plant* **2013**, *6*, 275–286. [[CrossRef](#)] [[PubMed](#)]
23. Wang, W.; Bai, X.D.; Chen, K.; Zhang, X.Y.; Gu, C.R.; Jiang, J.; Yang, C.P.; Liu, G.F. *PsnWRKY70* negatively regulates NaHCO<sub>3</sub> tolerance in *Populus*. *Int. J. Mol. Sci.* **2022**, *23*, 13086. [[CrossRef](#)] [[PubMed](#)]
24. Goodstein, D.M.; Shu, S.; Howson, R.; Neupane, R.; Hayes, R.D.; Fazo, J.; Mitros, T.; Dirks, W.; Hellsten, U.; Putnam, N.; et al. Phytozome: A comparative platform for green plant genomics. *Nucleic Acids Res.* **2012**, *40*, 1178–1186. [[CrossRef](#)]
25. Mistry, J.; Chuguransky, S.; Williams, L.; Qureshi, M.; Salazar, G.A.; Sonnhammer, E.; Tosatto, S.; Paladin, L.; Raj, S.; Richardson, L.J.; et al. Pfam: The protein families database in 2021. *Nucleic Acids Res.* **2021**, *49*, D412–D419. [[CrossRef](#)] [[PubMed](#)]
26. Duvaud, S.; Gabella, C.; Lisacek, F.; Stockinger, H.; Ioannidis, V.; Durinx, C. ExPasy, the Swiss Bioinformatics Resource Portal, as designed by its users. *Nucleic Acids Res.* **2021**, *49*, W216–W227. [[CrossRef](#)]
27. Chou, K.C.; Shen, H.B. Cell-PLoc: A package of Web servers for predicting subcellular localization of proteins in various organisms. *Nat. Protoc.* **2008**, *3*, 153–162. [[CrossRef](#)]
28. Chen, C.; Wu, Y.; Li, J.; Wang, X.; Zeng, Z.; Xu, J.; Liu, Y.; Feng, J.; Chen, H.; He, Y.; et al. TBtools-II: A “one for all, all for one” bioinformatics platform for biological big-data mining. *Mol. Plant* **2023**, *16*, 1733–1742. [[CrossRef](#)] [[PubMed](#)]
29. Chao, J.; Li, Z.; Sun, Y.; Aluko, O.O.; Wu, X.; Wang, Q.; Liu, G. MG2C: A user-friendly online tool for drawing genetic maps. *Mol. Hortic.* **2021**, *1*, 16–20. [[CrossRef](#)]
30. Tamura, K.; Stecher, G.; Kumar, S. MEGA11: Molecular evolutionary genetics analysis version 11. *Mol. Biol. Evol.* **2021**, *38*, 3022–3027. [[CrossRef](#)] [[PubMed](#)]
31. Guo, A.Y.; Zhu, Q.H.; Chen, X.; Luo, J.C. GSDS: A gene structure display server. *Yi Chuan* **2007**, *29*, 1023–1026. [[CrossRef](#)]



32. Bailey, T.L.; Williams, N.; Mischak, C.; Li, W.W. MEME: Discovering and analyzing DNA and protein sequence motifs. *Nucleic Acids Res.* **2006**, *34* (Suppl. 2), W369–W373. [[CrossRef](#)] [[PubMed](#)]
33. Lescot, M.; Dehais, P.; Thijs, G.; Marchal, K.; Moreau, Y.; Van de Peer, Y.; Rouze, P.; Rombauts, S. PlantCARE, a database of plant cis-acting regulatory elements and a portal to tools for in silico analysis of promoter sequences. *Nucleic Acids Res.* **2002**, *30*, 325–327. [[CrossRef](#)] [[PubMed](#)]
34. Blom, N.; Sicheritz-Ponten, T.; Gupta, R.; Gammeltoft, S.; Brunak, S. Prediction of post-translational glycosylation and phosphorylation of proteins from the amino acid sequence. *Proteomics* **2004**, *4*, 1633–1649. [[CrossRef](#)] [[PubMed](#)]
35. Love, M.I.; Huber, W.; Anders, S. Moderated estimation of fold change and dispersion for RNA-seq data with DESeq2. *Genome Biol.* **2014**, *15*, 550–571. [[CrossRef](#)]
36. Wu, X.; Yang, H.; Qu, C.; Xu, Z.; Li, W.; Hao, B.; Yang, C.; Sun, G.; Liu, G. Sequence and expression analysis of the AMT gene family in poplar. *Front. Plant Sci.* **2015**, *6*, 337. [[CrossRef](#)] [[PubMed](#)]
37. Lynch, M.; Conery, J.S. The evolutionary fate and consequences of duplicate genes. *Science* **2000**, *290*, 1151–1155. [[CrossRef](#)]
38. Kaya, C.; Ugurlar, F.; Adamakis, I.S. Molecular mechanisms of CBL-CIPK signaling pathway in plant abiotic stress tolerance and hormone crosstalk. *Int. J. Mol. Sci.* **2024**, *25*, 5043. [[CrossRef](#)]
39. Jacob, A.G.; Smith, C. Intron retention as a component of regulated gene expression programs. *Hum. Genet.* **2017**, *136*, 1043–1057. [[CrossRef](#)]
40. Hernandez-Garcia, C.M.; Finer, J.J. Identification and validation of promoters and cis-acting regulatory elements. *Plant Sci.* **2014**, *217–218*, 109–119. [[CrossRef](#)] [[PubMed](#)]
41. Zhou, L.; Lan, W.; Chen, B.; Fang, W.; Luan, S. A calcium sensor-regulated protein kinase, CALCINEURIN B-LIKE PROTEIN-INTERACTING PROTEIN KINASE19, is required for pollen tube growth and polarity. *Plant Physiol.* **2015**, *167*, 1351–1360. [[CrossRef](#)]
42. Luan, S. The CBL-CIPK network in plant calcium signaling. *Trends Plant Sci.* **2009**, *14*, 37–42. [[CrossRef](#)]
43. Fang, S.; Hou, X.; Liang, X. Response mechanisms of plants under Saline-Alkali stress. *Front. Plant Sci.* **2021**, *12*, 667458. [[CrossRef](#)]
44. Weinl, S.; Kudla, J. The CBL-CIPK Ca<sup>2+</sup>-decoding signaling network: Function and perspectives. *New Phytol.* **2009**, *184*, 517–528. [[CrossRef](#)] [[PubMed](#)]
45. Yu, Q.; An, L.; Li, W. The CBL-CIPK network mediates different signaling pathways in plants. *Plant Cell Rep.* **2014**, *33*, 203–214. [[CrossRef](#)]
46. Zhang, B.Q.; Song, X.P.; Zhang, X.Q.; Huang, Y.X.; Liang, Y.J.; Zhou, S.; Yang, C.F.; Yang, L.T.; Huang, X.; Li, Y.R. Differential gene expression analysis of *SoCBL* family calcineurin b-like proteins: Potential involvement in sugarcane cold stress. *Genes* **2022**, *13*, 246. [[CrossRef](#)]
47. Chen, Y.; Jin, Y.-F.; Wang, Y.; Gao, Y.; Wang, Q.; Xue, Y. Diverse roles of the CIPK gene family in transcription regulation and various biotic and abiotic stresses: A literature review and bibliometric study. *Front. Genet.* **2022**, *13*, 1041078. [[CrossRef](#)]
48. Barik, S. Special issue: Structure, function and evolution of protein domains. *Int. J. Mol. Sci.* **2022**, *23*, 6201. [[CrossRef](#)] [[PubMed](#)]
49. Mohanta, T.K.; Mohanta, N.; Mohanta, Y.K.; Parida, P.; Bae, H. Genome-wide identification of Calcineurin B-Like (CBL) gene family of plants reveals novel conserved motifs and evolutionary aspects in calcium signaling events. *BMC Plant Biol.* **2015**, *15*, 189. [[CrossRef](#)]
50. Ishitani, M.; Liu, J.; Halfter, U.; Kim, C.S.; Shi, W.; Zhu, J.K. SOS3 function in plant salt tolerance requires N-myristoylation and calcium binding. *Plant Cell* **2000**, *12*, 1667–1677. [[CrossRef](#)] [[PubMed](#)]
51. Zhou, X.; Hao, H.; Zhang, Y.; Bai, Y.; Zhu, W.; Qin, Y.; Yuan, F.; Zhao, F.; Wang, M.; Hu, J.; et al. SOS2-LIKE PROTEIN KINASE5, an SNF1-RELATED PROTEIN KINASE3-Type protein kinase, is important for abscisic acid responses in *Arabidopsis* through phosphorylation of ABSCISIC ACID-INSENSITIVE5. *Plant Physiol.* **2015**, *168*, 659–676. [[CrossRef](#)]
52. Mao, J.; Manik, S.M.; Shi, S.; Chao, J.; Jin, Y.; Wang, Q.; Liu, H. Mechanisms and physiological roles of the CBL-CIPK networking system in *Arabidopsis thaliana*. *Genes* **2016**, *7*, 62. [[CrossRef](#)] [[PubMed](#)]
53. Batic, O.; Kudla, J. Analysis of calcium signaling pathways in plants. *Biochim. Biophys. Acta* **2012**, *1820*, 1283–1293. [[CrossRef](#)] [[PubMed](#)]
54. Drerup, M.M.; Schlucking, K.; Hashimoto, K.; Manishankar, P.; Steinhorst, L.; Kuchitsu, K.; Kudla, J. The Calcineurin B-like calcium sensors CBL1 and CBL9 together with their interacting protein kinase CIPK26 regulate the *Arabidopsis* NADPH oxidase RBOHF. *Mol. Plant* **2013**, *6*, 559–569. [[CrossRef](#)] [[PubMed](#)]
55. Zhang, H.; Lv, F.; Han, X.; Xia, X.; Yin, W. The calcium sensor PeCBL1, interacting with PeCIPK24/25 and PeCIPK26, regulates Na<sup>+</sup>/K<sup>+</sup> homeostasis in *Populus euphratica*. *Plant Cell Rep.* **2013**, *32*, 611–621. [[CrossRef](#)] [[PubMed](#)]
56. Egea, I.; Pineda, B.; Ortiz-Atienza, A.; Plasencia, F.A.; Drevensek, S.; Garcia-Sogo, B.; Yuste-Lisbona, F.J.; Barrero-Gil, J.; Amares, A.; Flores, F.B.; et al. The SICBL10 Calcineurin B-Like protein ensures plant growth under salt stress by regulating Na<sup>+</sup> and Ca<sup>2+</sup> homeostasis. *Plant Physiol.* **2018**, *176*, 1676–1693. [[CrossRef](#)]

57. Liu, F.; Liu, Q.; Wu, J.H.; Wang, Z.Q.; Geng, Y.J.; Li, J.; Zhang, Y.; Li, S. Arabidopsis calcineurin B-like-interacting protein kinase 8 and its functional homolog in tomato negatively regulates ABA-mediated stomatal movement and drought tolerance. *Plant Cell Environ.* **2024**, *47*, 2394–2407. [[CrossRef](#)]
58. Wang, L.; Feng, X.; Yao, L.; Ding, C.; Lei, L.; Hao, X.; Li, N.; Zeng, J.; Yang, Y.; Wang, X. Characterization of CBL-CIPK signaling complexes and their involvement in cold response in tea plant. *Plant Physiol. Biochem.* **2020**, *154*, 195–203. [[CrossRef](#)]
59. Chuamnakhong, S.; Nampei, M.; Ueda, A. Characterization of Na<sup>+</sup> exclusion mechanism in rice under saline-alkaline stress conditions. *Plant Sci.* **2019**, *287*, 110171. [[CrossRef](#)]
60. Yang, Y.; Zhang, C.; Tang, R.J.; Xu, H.X.; Lan, W.Z.; Zhao, F.; Luan, S. Calcineurin B-Like proteins CBL4 and CBL10 mediate two independent salt tolerance pathways in *Arabidopsis*. *Int. J. Mol. Sci.* **2019**, *20*, 2421. [[CrossRef](#)] [[PubMed](#)]

**Disclaimer/Publisher's Note:** The statements, opinions and data contained in all publications are solely those of the individual author(s) and contributor(s) and not of MDPI and/or the editor(s). MDPI and/or the editor(s) disclaim responsibility for any injury to people or property resulting from any ideas, methods, instructions or products referred to in the content.